Ocean Engineering 104 (2015) 558–567

Contents lists available at ScienceDirect

Ocean Engineering

journal homepage: www.elsevier.com/locate/oceaneng

Adaptive neural path-following control for underactuated ships in fields of marine practice

Guoqing Zhang, Xianku Zhang *, Yunfeng Zheng

Navigation College, Dalian Maritime University, Dalian 116026 Liaoning, People's Republic of China

ARTICLE INFO

Article history:
Received 1 November 2013
Accepted 15 May 2015
Available online 18 June 2015

Keywords:
Underactuated ships
Path following
Adaptive control
Guidance system
Neural networks

ABSTRACT

In this note, one concerns with the problem of robust adaptive path-following control for uncertain underactuated ships in fields of marine practice: waypoints based navigation. A novel "logical virtual ship (LVS)" based steering law is developed to programme the rational reference route, which is to guidance the underactuated ship in the practical engineering. Furthermore, a practical adaptive neural control algorithm is proposed by virtue of the dynamic surface control (DSC) technique, neural networks approximation and polar coordinates scheme. And much effort are made to obtain semi-global uniform ultimate bounded stability for the closed-loop control system, using the Lyapunov synthesis. The advantages of the developed control scheme are that first, it could tackle the practical condition "waypoints based navigation", which is very meaningful for applying the existed theoretical algorithm in control engineering; second, the developed neural controller is able to capture the vehicle uncertainties without the exact information of hydrodynamic damping structure and the sea disturbances. These characteristics would facilitate the implementation of the algorithm in the marine practice. Two numerical examples have been given to illustrate the performance and effectiveness of the proposed scheme.

1. Introduction

Ocean surface ship is one example of underactuated mechanical systems (Jiang, 2011). Over the last few years, controlling underactuated surface ships has been an active research field due to its theoretical challenges and important applications such as passenger and cargo transportation. Most ocean vessels are underactuated meaning that they are equipped with propellers and rudders for surge and yaw motions only, while without any actuators for direct control of sway motion. Even though state-of-the-art actuation systems, such as tunnel thrusters and azipods, are equipped, it is ineffective to provide actuation in the sway direction at high speeds.

According to the Brockett necessary condition, underactuated ships cannot be stabilized by the time-invariant continuous control law though it is open loop controllable (Do and Pan, 2009; Brockett et al., 1983). Several authors have contributed a set of novel ideas and strategies, mainly including time-varying feedback (Pettersen and Nijmeijer, 2001; Do et al., 2004; Do, 2010) and discontinuous feedback (Ghommam et al., 2006; Liu et al., 2012) methods. Pettersen and Nijmeijer (2001) applied the recursive technique to provide a high gain based local exponential stabilization result. Under sufficient conditions of persistent excitation, the global tracking problem for underactuated ship was studied in Jiang (2002). Two constructive tracking solutions were proposed by application of Lyapunov's direct method. However, it is noted that in Pettersen and Nijmeijer (2001) and Jiang (2002) the yaw velocity was assumed to be nonzero. The assumption implies that the reference trajectory cannot be straight line. In order to dispose this problem, Do et al. (2004) used a transformation between ψ_e and (ψ, x_e, y_e). A nonlinear robust adaptive algorithm was developed to force an underactuated ship to follow a predefined path at a desired speed, considering the presence of the external disturbances. The related techniques included Lyapunov's direct method, Backstepping technique and parameter projection algorithm. In Ghommam et al. (2006), the authors transformed the whole dynamical system into a cascade nonlinear system using two steps, and then derived a time-invariant discontinuous feedback law to exponentially stabilize the plant based on the backstepping approach. The controllers for $\psi(0) \neq 0$ and $\psi(0) = 0$ were designed. Robust adaptive tracking control of fully actuated ocean surface vessels has been studied in Chen et al. (2009), Tee and Ge (2006), and Chen et al. (2010a). In the research, neural networks (NNs) approximation and Backstepping techniques were used to tackle system uncertainties and an auxiliary design system was introduced to deal with the impact

* Corresponding author. Tel.: +86 41184729572.
E-mail addresses: zgq_dlmu@163.com (G. Zhang), zhangxk@dlmu.edu.cn (X. Zhang), zyfxyn@sohu.com (Y. Zheng).

http://dx.doi.org/10.1016/j.oceaneng.2015.05.013
0029-8018/

of control input saturation. Simulation results have illustrated the effectiveness of the control law. K.D. Do provided his recent research achievements "Practical control of underactuated ships" in Do (2010). The achieved control objective is global practical stabilization of arbitrary reference trajectories, including fixed points and nonadmissible trajectories.

However, a common assumption in the aforementioned literatures around controlling underactuated ships is that the uncertainty is only in the linearly parameterized form. That is, the model nonlinearities are assumed to be known while the linearized parameters are unknown. That is not in accordance with the marine control engineering. There exist both the parametric uncertainty and unknown hydrodynamic structure for the control design. To cope with such nonlinear arbitrary uncertainties, the control task of underactuated ships is attended using the idea of adaptive backstepping with neural networks or T–S fuzzy system based approximation (Wang and Huang, 2005; Li et al., 2010, 2012; Tong et al., 2010). Another theoretical obstruction is the problem "explosion of complexity" that is inherent in the Backstepping technique (Krstic et al., 1995). It is caused by repeated differentiations of virtual controls, which is impossible to implement in practice and poses the burden-some problem. Fortunately, DSC technique has been presented in Li et al. (2010) and Yang and Wang (2007) to tackle this problem by introducing a first-order low-pass filter in the conventional backstepping design. Combining Backstepping method, radial basis function neural networks and "minimal learning parameter" technique, a robust adaptive tracking control approach was proposed for a class of strict-feedback nonlinear systems. Though, the above techniques cannot directly be applied to the underactuated vehicle for its underactuated constraint and the strong couplings among the different DOFs (degree of freedom).

In this note, motivated by the above-mentioned observations, a practical adaptive neural path-following control scheme, which is performed by using a novel guidance steering law "LVS", NNs approximation, DSC technique, is developed for underactuated ships without knowing the exact information of the hydrodynamic forces/moments (i.e. the model uncertainties include the terms related to the parameter and the unknown structure) and the marine environment disturbances. The main contributions of this note can be summarized as follows:

(1) By virtue of the idea "logical virtual ship", a novel guidance steering law is first developed to tackle the marine practical condition: the reference route generated by the waypoints. That is critical and important for applying these existed path-following algorithms in the control engineering. To the best of the authors' knowledge, few similar result has been presented in the literatures.
(2) The developed robust adaptive controller is universal and model independent, and the problem "explosion of complexity" is avoided for the merit of the DSC technique. While those developed in Li et al. (2008) and Breivik et al. (2008) are not suitable in practice.
(3) With the special property and structure of our scheme, the potential controller singularity problem existing in many adaptive control algorithm is avoided.

The rest of this paper is organized as follows. In Section 2, mathematical model and problem formulation are given. Section 3 is devoted to a systematic procedure for the proposed controller. In Section 4, analysis of system stability and performance of the controller are formulated. In Section 5, some numerical simulations are given to illustrate the effectiveness of the proposed approach. Section 6 contains the conclusion.

2. Problem formulation and preliminaries

2.1. Problem formulation

By use of Newtonian or Lagrangian mechanics (Fossen, 2011), the mathematical model of underactuated ships with three degrees of freedom (neglecting motions in heave, pitch and roll) is described in the following equation:

$$\begin{aligned}
&\dot{x} = u\cos(\psi) - v\sin(\psi),\\
&\dot{y} = u\sin(\psi) + v\cos(\psi),\\
&\dot{\psi} = r,\\
&\dot{u} = f_u(\overline{v}) + \frac{1}{m_u}\tau_u + \frac{1}{m_u}\tau_{wu}(t),\\
&\dot{v} = f_v(\overline{v}) + \frac{1}{m_v}\tau_{wv}(t),\\
&\dot{r} = f_r(\overline{v}) + \frac{1}{m_r}\tau_r + \frac{1}{m_r}\tau_{wr}(t)
\end{aligned} \tag{1}$$

with

$$\begin{aligned}
f_u(\overline{v}) &= \frac{m_v}{m_u}vr - \frac{d_u}{m_u}u - \frac{d_{u2}}{m_u}|u|u - \frac{d_{u3}}{m_u}u^3,\\
f_v(\overline{v}) &= -\frac{m_u}{m_v}ur - \frac{d_v}{m_v}v - \frac{d_{v2}}{m_v}|v|v - \frac{d_{v3}}{m_v}v^3,\\
f_r(\overline{v}) &= \frac{(m_u - m_v)}{m_r}uv - \frac{d_r}{m_r}r - \frac{d_{r2}}{m_r}|r|r - \frac{d_{r3}}{m_{33}}r^3
\end{aligned}$$

where (x, y, ψ) are the surge, sway displacement and yaw angle in the earth-fixed coordinate frame, respectively, and $\overline{v} = [u, v, r]^{\mathrm{T}}$ denotes the surge, sway and yaw velocities, respectively. Based on the physical consideration, the yaw angle ψ is just defined in domain of $[0, 2\pi)$. (τ_u, τ_r) are the control inputs: the surge force and yaw moment. $(\tau_{wu}, \tau_{wv}, \tau_{wr})$ are used to describe immeasurable environmental disturbance forces and moments due to waves, wind and ocean current, respectively. $m_u, m_v, m_r, d_u, d_v, d_r, d_{u2}, d_{v2}, d_{r2}, d_{u3}, d_{v3}, d_{r3}$ are all considered as unknown parameters, and describe the ship's inertia, hydrodynamic damping, and nonlinear damping terms. The unknown nonlinear functions $f_u(\overline{v}), f_v(\overline{v}), f_r(\overline{v})$ denote the nonlinear structure uncertainties in the mathematical model.

Control objective: Note, the practical conditions considered in this note include waypoints based navigation, unknown hydrodynamic terms and unmodeled dynamics, the marine environment disturbance. The control objective is to develop an adaptive neural path-following control scheme (consist of the LVS guidance law, the surge force τ_u and the yaw moment τ_r) to tackle the above mentioned obstructions, such that the underactuated ship (1) follows closely the specified reference path AB (see Fig. 1). All state variables of the underactuated ship are semi-global uniform ultimate bounded (SGUUB).

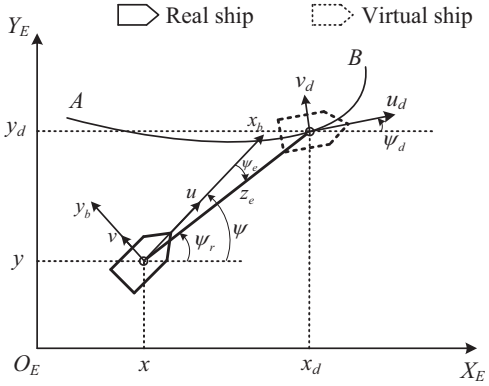

Fig. 1. General framework for path-following control.

Assumption 1. The reference path is generated by a virtual ship (2), which is regular and smooth enough. $x_d, \dot{x}_d, \ddot{x}_d, y_d, \dot{y}_d, \ddot{y}_d$ and $\psi_d, \dot{\psi}_d$ exist and are bounded:

$$\begin{aligned}\dot{x}_d &= u_d \cos(\psi_d),\\ \dot{y}_d &= u_d \sin(\psi_d),\\ \dot{\psi}_d &= r_d\end{aligned} \tag{2}$$

where all variables have similar meanings to (1) and $\psi_d \in [0, 2\pi)$.

Remark 1. Assumption 1 is a common precondition for path-following control in the existing literatures. However, the reference path or trajectory is usually generated by waypoints in the marine practice. For this case, a novel guidance system will be detailed in Section 3.1.

Assumption 2. Assume that the environmental disturbance terms satisfy $|\tau_{wu}| \le \tau_{wu\,\max}, |\tau_{wv}| \le \tau_{wv\,\max}, |\tau_{wr}| \le \tau_{wr}\max$, where $\tau_{wu}\max, \tau_{wv}\max$ and $\tau_{wr}\max$ are unknown positive constants.

Definition 1. Consider the system with the general form $\dot{x}_i = f(X) + d$, $X = [x_1, x_2, \ldots, x_n]^{\mathrm{T}}$, $f: R^n \to R$ is a function and d denotes the disturbance. For the bounded variable $x_j, j \neq i$ and d, if there exists a Lyapunov candidate $V(x_i) \in C^1$ satisfying

(1) $V(x_i)$ is globally positive definite and radially unbounded.
(2) $\dot{V}(x_i) < 0$ if $|x_i| > \bar{x}_i^*$, $\bar{x}_i^*$ is a positive constant and is related to the bounds of $x_j, j \neq i$ and d.

the state variable x_i is referred as passive-bounded stable.

Assumption 3. The sway velocity v is passive-bounded stable, following Do et al. (2004) and Li et al. (2008).

Remark 2. The passive-boundedness of the sway dynamic has been systematically analyzed considering different cases in Li et al. (2008). This assumption is reasonable in marine navigation practice.

In addition, this note only concerns with the state feedback control task, i.e. one assumes that the states are available or they need to be estimated using an observer in practical situations.

2.2. Nonlinear function approximation

Function approximation is recalled in this section, which may be nonlinearly or linearly parameterized. In control engineering, examples of nonlinear function approximators include NNs (Wang and Huang, 2005; Li et al., 2010; Tee and Ge, 2006; Ge and Wang, 2002; Peng et al., 2010) and adaptive fuzzy systems (Yang and Zhou, 2005; Ting, 2009). In this note, we introduce RBF NNs in the proposed control scheme to deal with the model uncertainties. For any given real continuous function $f(\bar{x})$ with $f(0) = 0$, the networks can be written as follows:

$$f_{nn}(\bar{x}) = \boldsymbol{W}^{\mathrm{T}} \boldsymbol{S}(\bar{x}) + \varepsilon \tag{3}$$

where the input vector $\bar{x} \in \Omega_{\bar{x}}$, and $\Omega_{\bar{x}}$ is a compact set in R^m. $\boldsymbol{W} = [w_1, w_2, \ldots, w_l]^{\mathrm{T}} \in R^l$ is the adaptable weight vector, $\boldsymbol{S}(\bar{x}) = [s_1(\bar{x}), s_2(\bar{x}), \ldots, s_l(\bar{x})]$ is a vector of RBF basis functions with the form of Gaussian functions (4). ε is the approximation error with unknown upper bound $\bar{\varepsilon}$, $l > 1$ is the node number of NNs, m is the dimension number of $\bar{x}$.

$$s_i(\bar{x}) = \xi_j \exp\left[\frac{-(\bar{x} - \boldsymbol{\mu}_j)^{\mathrm{T}}(\bar{x} - \boldsymbol{\mu}_j)}{2\eta_j^2}\right], \quad j = 1, 2, \ldots, l \tag{4}$$

where ξ_j is the gain coefficient, $\boldsymbol{\mu}_j = [\mu_{j1}, \mu_{j2}, \ldots, \mu_{jm}]^{\mathrm{T}}$ is the center of the receptive field and η_j is the width of the Gaussian function.

According to Ge and Wang (2002), it has been proven that $f_{nn}(\bar{x})$ can be approximated over a compact set $\Omega_{\bar{x}} \subset R^m$ to arbitrary any accuracy with the ideal constant weights:

$$\boldsymbol{W}^{*\mathrm{T}} := \arg\min_{\boldsymbol{W} \in R^l} \left\{ \sup_{\bar{x} \in \Omega_{\bar{x}}} \left| f_n(\bar{x}) - \boldsymbol{W}^{\mathrm{T}} \boldsymbol{S}(\bar{x}) \right| \right\} \tag{5}$$

Throughout the paper, $|\cdot|$ is the absolute operator. $\|\cdot\|$ denotes the Euclidean norm, $\|\cdot\|^2 = \sum_{i,j}\{\}_{i,j}^2$. $(\cdot)_{i,j}$ denotes the element of $(\cdot)$ in row i and column j. $\hat{(\cdot)}$ is the estimate of $(\cdot)$, and the estimation error $\tilde{(\cdot)} = \hat{(\cdot)} - (\cdot)$.

3. Design of adaptive neural path-following control

In order to accomplish the path-following control design in fields of marine practice, a novel guidance system is presented based on the virtual ship in Section 3.1, and then one develop a adaptive neural control law for underactuated ships (1) under Assumptions 1–3. The design procedure contains two steps: for kinematic control and for kinetic control.

3.1. Guidance system for underactuated ships

Guidance systems for marine vessels have been detailed in Fossen (2011). For path-following in case of straight-line paths, line-of-sight (LOS) steering law is used to derive the desired heading angle ψ_d, and then the control object $\psi \to \psi_d$ can be guaranteed by a heading autopilot (Khaled and Chalhoub, 2013). However, no one guidance steering law is suited to waypoints based path generating for underactuated ships, and few result is presented in the current literatures.

In marine navigation practice, the reference path is usually generated by waypoints $W_1, W_2, \ldots, W_n$ with $W_i = (x_i, y_i)$, which guide the vessel moving in the open sea (Fossen, 1998). For this purpose, a novel guidance system law is developed by splitting the reference path into regular straight lines and smooth arcs, which can be generated by a virtual ship (2), see Fig. 2. The object is to obtain the input orders u_d, r_d and the corresponding time t_d. In Fig. 2, the desired trajectory of the virtual ship is $W_{i-1} \to P_{\mathrm{in}Wi} \to arc \to P_{\mathrm{out}Wi} \to W_{i+1}$. Normally, u_d is a positive constant determined by the operator, while r_d is a order changing over time. In the straight lines $W_{i-1}P_{\mathrm{in}Wi}$ and $P_{\mathrm{out}Wi}W_{i+1}$, $r_d = 0, t_d = distance/u_d$. In the smooth arcs $P_{\mathrm{in}Wi}P_{\mathrm{out}Wi}$, r_d is a non-zero constant that can be calculated for the virtual ship being without any inertia and uncertainties. Firstly, the angle of $W_{i-1}W_i$ can be obtained from (6), and the angle $\Delta\phi_i$ is defined by $\Delta\phi_i = \phi_{i,i+1} - \phi_{i-1,i}$. The turning radius R_i, resting with $|\Delta\phi_i|$ in $(0, \pi/2]$, is determined by interpolation in $[R_{\min}, R_{\max}]$. It is noted that the parameter setting of $R_{\min}, R_{\max}$ depends on the ship maneuvering

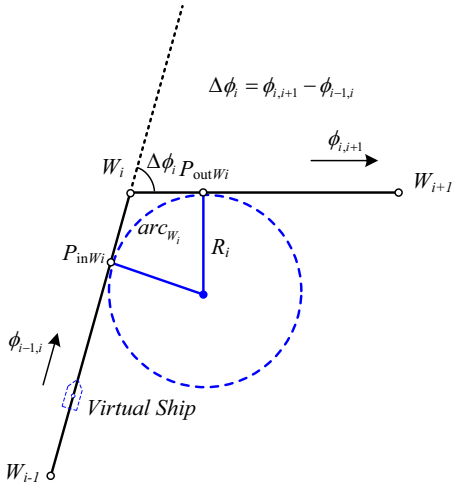

Fig. 2. Waypoints based path generation frame for underactuated ships.

performance. Especially, the appropriate selection of $R_{\min}$ could avoid or reduce the effect of saturation. If $|\Delta\phi_i| > \pi/2$, $R_i = R_{\min}$. Then the r_d, t_d in arc $P_{\text{inW}i}P_{\text{outW}i}$ can be easily obtained by $r_d = u_d/R_i$, $t_d = \Delta\phi_i/r_d$. A similar procedure is employed repeatedly for each waypoint, and finally the reference path generation is completed. Based on the above derivation, the logical computing is the key role of the novel guidance steering law. That is the original intent of "LVS":

$$\phi_{i-1,i} = \arctan\frac{y_i - y_{i-1}}{x_i - x_{i-1}} \tag{6}$$

3.2. Control design

Step 1: According to transformation under polar coordinates, the path-following error variables are defined as follows, refer to Fig. 1:

$$\begin{aligned} &x_e = x_d - x, \quad y_e = y_d - y, \\ &\psi_e = \psi_r - \psi, \quad z_e = \sqrt{x_e^2 + y_e^2} \end{aligned} \tag{7}$$

where

$$\psi_r = \begin{cases} \left[1 - 0.5(1+\text{sgn}(x_e))\,\text{sgn}(y_e)\right]\cdot\pi + \arctan\left(\dfrac{y_e}{x_e}\right), & z_e \neq 0 \\ \psi_d, & z_e = 0 \end{cases} \tag{8}$$

It is noted that $\psi_r(\psi_r \in [0, 2\pi))$ is the ship's azimuth angle relative to the virtual ship, while not yaw angle ψ_d of the virtual ship. In fact, the intention of the transformation for case $z_e \neq 0$ is to place $\arctan(y_e/x_e)$ in the definition domain $[0, 2\pi)$, which is complete for describing the angle variable in the ocean engineering. In Eq. (8), $\arctan(y_e/x_e)$ is not defined at $z_e = 0$. Thus, one sets $\psi_r = \psi_d$ when $z_e = 0$. That guarantees that the ship closely follows the virtual one in terms of both position and orientation. Hence, the variable ψ_r is continuous in the domain $[0, \pi)$.

Referring to Fig. 1, we can get the following equation:

$$x_e = z_e\cos(\psi_r), \quad y_e = z_e\sin(\psi_r) \tag{9}$$

Furthermore, $\dot{z}_e$ and $\dot{\psi}_e$ can be derived along with (1), (7), (9):

$$\begin{aligned} &\dot{z}_e = \dot{x}_d\cos\psi_r + \dot{y}_d\sin\psi_r - u\cos\psi_e - v\sin\psi_e \\ &\dot{\psi}_e = \dot{\psi}_r - r \end{aligned} \tag{10}$$

then two desired virtual control inputs for u and r are chosen as

$$\begin{aligned} &\alpha_u = \frac{k_{ze}(z_e - \delta_m) + \dot{x}_d\cos\psi_r + \dot{y}_d\sin\psi_r - v\sin\psi_e}{\cos\psi_e} \\ &\alpha_r = k_{\psi e}\psi_e + \dot{\psi}_r \end{aligned} \tag{11}$$

where $k_{ze} > 0$ and $k_{\psi e} > 0$ are design parameters. Note that the α_u is not defined when $\psi_e = \pm\pi/2$. Therefore, $|\psi_e| < \pi/2$ is required in the control design, and (12) is incorporated to implement the virtual control law α_u in the practical engineering. In each control cycle, Eq. (12) is applied to the error variable ψ_e until it locates in the enable domain $(-\pi/2, \pi/2)$. Note, the transformation (12) does not change the virtual control direction and the derived control law α_u also desires to stabilize the $z_e - \delta_m$ to zero. δ_m is a small positive value. In α_u, $(z_e - \delta_m)$ instead of z_e is used to guarantee that the real ship is usually following behind the virtual one that will facilitate satisfying the condition $|\psi_e| < \pi/2$. Consequently, the error variable z_e satisfies $\lim_{t\to\infty} z_e = \delta_m$. Eq. (8) guarantees that ψ_r moves continuously in $[0, \pi)$. In the expression of α_r, $\dot{\psi}_r$ is obtained by fuse of the discrete transformation $\dot{\psi}_r = (\psi_r(t) - \psi_r(t-1))/\Delta t$ instead of the analytical method, where Δt is signal measuring instant. That is common for calculating the differential term in control engineering. For special cases, some additional transformations also require to be conducted to calculate the variable $\dot{\psi}_r$. E.g., if $\psi_r(t-1) = 0^\circ, \psi_r(t) = 359.5^\circ$, $\dot{\psi}_r = (\psi_r(t) - \psi_r(t-1) - 360^\circ)/\Delta t = -0.5^\circ/\Delta t$:

$$\psi_e = \begin{cases} \psi_e - \pi, & \psi_e \geq \pi/2 \\ \psi_e, & -\pi/2 < \psi_e < \pi/2 \\ \psi_e + \pi, & \psi_e \leq -\pi/2 \end{cases} \tag{12}$$

Before the next step, the DSC technique is employed here to solve the so-called "explosion of complexity". Two new state variables β_u and β_r are introduced, and let α_u and α_r pass through a first-order filter (dynamic surface) with time constants ϵ_u and ϵ_r, respectively:

$$\begin{aligned} &\epsilon_u\dot{\beta}_u + \beta_u = \alpha_u, \quad \beta_u(0) = \alpha_u(0), \quad y_u = \alpha_u - \beta_u \\ &\epsilon_r\dot{\beta}_r + \beta_r = \alpha_r, \quad \beta_r(0) = \alpha_r(0), \quad y_r = \alpha_r - \beta_r \end{aligned} \tag{13}$$

The time derivative $\dot{y}_i, i = u, r$ along (11), (13) is derived:

$$\begin{aligned} \dot{y}_u &= \dot{\alpha}_u - \dot{\beta}_u \\ &= \frac{\partial\alpha_u}{\partial x}\dot{x} + \frac{\partial\alpha_u}{\partial y}\dot{y} + \frac{\partial\alpha_u}{\partial\psi}\dot{\psi} + \frac{\partial\alpha_u}{\partial x_d}\dot{x}_d + \frac{\partial\alpha_u}{\partial y_d}\dot{y}_d \\ &\quad + \frac{\partial\alpha_u}{\partial\psi_r}\dot{\psi}_r + \frac{\partial\alpha_u}{\partial\dot{x}_d}\ddot{x}_d + \frac{\partial\alpha_u}{\partial\dot{y}_d}\ddot{y}_d + \frac{\partial\alpha_u}{\partial v}\dot{v} - \frac{y_u}{\epsilon_u} \\ &= B_u(\cdot) - \frac{y_u}{\epsilon_u} \\ \dot{y}_r &= \dot{\alpha}_r - \dot{\beta}_r \\ &= \frac{\partial\alpha_r}{\partial\psi}\dot{\psi} + \frac{\partial\alpha_r}{\partial\psi_r}\dot{\psi}_r + \frac{\partial\alpha_r}{\partial\dot{\psi}_r}\ddot{\psi}_r - \frac{y_r}{\epsilon_r} \\ &= B_r(\cdot) - \frac{y_r}{\epsilon_r} \end{aligned} \tag{14}$$

where $B_u(\cdot), B_r(\cdot)$ are continuous functions.

Step 2: Define the error variables $u_e = \beta_u - u, r_e = \beta_r - r$ and take their time derivative as follows:

$$\begin{aligned} &\dot{u}_e = \dot{\beta}_u - f_u(\overline{v}) - \frac{1}{m_u}\tau_u - \frac{1}{m_u}\tau_{wu}(t) \\ &\dot{r}_e = \dot{\beta}_r - f_r(\overline{v}) - \frac{1}{m_r}\tau_r - \frac{1}{m_r}\tau_{wr}(t) \end{aligned} \tag{15}$$

Let

$$\begin{aligned} &f_{nu}(\boldsymbol{Z}_u) = \dot{\beta}_u - f_u(\overline{v}) \\ &f_{nr}(\boldsymbol{Z}_r) = \dot{\beta}_r - f_r(\overline{v}) \end{aligned}$$

and they can be approximated by NNs as (3). The input vectors are $\boldsymbol{Z}_u = [-y_u/\epsilon_u, u, v, r]^{\mathrm{T}}, \boldsymbol{Z}_r = [-y_r/\epsilon_r, u, v, r]^{\mathrm{T}}$. The dynamic of the errors system (15) is given by (16). In our case, the orders of RBF networks are selected as $l = 25, m = 4$:

$$\begin{aligned} &\dot{u}_e = \boldsymbol{W}_u^{\mathrm{T}}\boldsymbol{S}(\boldsymbol{Z}_u) - \frac{1}{m_u}\tau_u + \varepsilon_u - \frac{1}{m_u}\tau_{wu}(t) \\ &\dot{r}_e = \boldsymbol{W}_r^{\mathrm{T}}\boldsymbol{S}(\boldsymbol{Z}_r) - \frac{1}{m_r}\tau_r + \varepsilon_r - \frac{1}{m_r}\tau_{wr}(t) \end{aligned} \tag{16}$$

The corresponding control law is chosen as

$$\begin{aligned} &\tau_u = k_{ue}u_e + \hat{\boldsymbol{W}}_u^{\mathrm{T}}\boldsymbol{S}_u + \frac{\hat{\tau}_{wu\,\max}u_e}{4\delta_u} \\ &\tau_r = k_{re}r_e + \hat{\boldsymbol{W}}_r^{\mathrm{T}}\boldsymbol{S}_r + \frac{\hat{\tau}_{wr\,\max}r_e}{4\delta_r} \end{aligned} \tag{17}$$

As to the approximator, one follows the method proposed in Chen et al. (2010a) to identify the RBF NNs. It is with the advantage for its concise form and robustness, and was commonly employed in the engineering-considered works. Finally, the update law for the NNs weights and the estimated upper bound of external disturbances are taken to be

$$\begin{aligned} &\dot{\hat{\boldsymbol{W}}}_u = \Gamma_u\left[\boldsymbol{S}_u u_e - \sigma_u\left(\hat{\boldsymbol{W}}_u - \hat{\boldsymbol{W}}_u(0)\right)\right] \\ &\dot{\hat{\boldsymbol{W}}}_r = \Gamma_r\left[\boldsymbol{S}_r r_e - \sigma_r\left(\hat{\boldsymbol{W}}_r - \hat{\boldsymbol{W}}_r(0)\right)\right] \end{aligned}$$

$$\dot{\hat{\tau}}_{wu\,\max}=\gamma_{wu}\left[\frac{u_e^2}{4\delta_u}-\sigma_{wu}(\hat{\tau}_{wu\,\max}-\hat{\tau}_{wu\,\max}(0))\right]$$
$$\dot{\hat{\tau}}_{wr\,\max}=\gamma_{wr}\left[\frac{r_e^2}{4\delta_r}-\sigma_{wr}(\hat{\tau}_{wr\,\max}-\hat{\tau}_{wr\,\max}(0))\right] \tag{18}$$

In (17) and (18), $k_{ue}, k_{re}, \delta_u, \delta_r, \Gamma_u, \Gamma_r, \gamma_u, \gamma_r, \sigma_u, \sigma_r, \sigma_{wu}, \sigma_{wr}$ are positive design parameters. $\hat{\boldsymbol{W}}_u(0)$, $\hat{\boldsymbol{W}}_r(0)$, $\hat{\tau}_{wu\,\max}(0)$, $\hat{\tau}_{wr\,\max}(0)$ are the initial value of the related variables.

Remark 3. Compared with the previous works in Do and Pan (2009), Do (2010), and Ghommam et al. (2010), it can be observed from the expressions of the control efforts τ_u, τ_r in (17) that the proposed algorithm does not require the information around the hydrodynamic terms, unmodeled dynamics due to the online approximation capability of NNs. By virtue of the DSC technique, the re-derivative of the virtual control is disposed. In addition, although the disturbance bounds mentioned in Assumption 2 are assumed to exist, they are not presented in the control (18) and do not have to be known. The above consideration leads to a control law with concise form, and it is easy to implement in real engineering.

Furthermore, it is noted that the NNs are only incorporated to tackle the unknown system function $f_{nu}(\mathbf{Z}_u), f_{nr}(\mathbf{Z}_r)$ in (16). The unknown control gain coefficients $1/m_u, 1/m_r$ are not required to be estimated. Thus, the potential control singularity problem is avoided, which usually exists in many feedback linearization adaptive control (Ge et al., 2001).

4. Stability analysis

Based on the controller design, the main result of this note is summarized as Theorem 1.

Theorem 1. *Consider the closed-loop system consisting of the underactuated ship (1) satisfying Assumptions 1–3, the adaptive neural control law (17) and adaptive laws (18). Then for bounded initial conditions, one can tune the controller parameters k_{ze}, k_{ψ_e}, k_{ue}, k_{re}, Γ_u, Γ_r, σ_u, σ_r, γ_{wu}, γ_{wr}, σ_{wu}, σ_{wr}, δ_u, δ_r, ϵ_u and ϵ_r such that all signals in the closed-loop system are semi-global uniform ultimate bounded (SGUUB), and the vector $\boldsymbol{Z}=[z_e-\delta_m, \psi_e, y_u, y_r, u_e, r_e, \tilde{W}_u, \tilde{W}_r, \tilde{\tau}_{wu\,\max}, \tilde{\tau}_{wr\,\max}]$ remains in the compact set:*

$$\Omega_{\boldsymbol{Z}}:=\Big\{\boldsymbol{Z}\,|\,(z_e-\delta_m)^2+\psi_e^2+y_u^2+y_r^2+u_e^2+r_e^2\le C_0, \|\tilde{\boldsymbol{W}}_i\|^2\le\frac{C_0}{\lambda_{\min}(\Gamma_i^{-1})}, \tilde{\tau}_{wi\max}^2\le\frac{C_0}{\gamma_{wi}^{-1}},\ i=u,r\Big\} \tag{19}$$

where $C_0>0$ is a constant.

Proof. Considering the following Lyapunov function candidate:

$$V=\tfrac{1}{2}(z_e-\delta_m)^2+\tfrac{1}{2}\psi_e^2+\tfrac{1}{2}y_u^2+\tfrac{1}{2}y_r^2+\tfrac{1}{2}m_uu_e^2+\tfrac{1}{2}m_rr_e^2+\tfrac{1}{2}\left[\tilde{\boldsymbol{W}}_u^{\mathrm{T}}\Gamma_u^{-1}\tilde{\boldsymbol{W}}_u+\tilde{\boldsymbol{W}}_r^{\mathrm{T}}\Gamma_r^{-1}\tilde{\boldsymbol{W}}_r+\gamma_{wu}^{-1}\tilde{\tau}_{wu\,\max}^2+\gamma_{wr}^{-1}\tilde{\tau}_{wr\,\max}^2\right] \tag{20}$$

It should be mentioned that the NNs introduced in (17) always remain good approximation capability on the suitable compact set. However, the stable performance cannot be guaranteed once the input vector is out of the compact set. That is why the stability of the closed-loop system obtained in this note is only semiglobal instead of global. In fact, it is still an open problem that how to identify the compact set and obtain the global stability by use of the approximation based control schemes (Chen et al., 2010b; Chen and Jiao, 2010). Thus, we still assume that the states $(\dot{x}_d, \ddot{x}_d, \dot{y}_d, \ddot{y}_d, z_e, \dot{z}_e, \psi_r, \dot{\psi}_r, \ddot{\psi}_r, \psi_e, \dot{\psi}_e, \ddot{\psi}_e, v, \dot{v})$ always remain within the compact set, and there exist positive constants M_u and M_r such that $|B_u(\cdot)|\le M_u, |B_r(\cdot)|\le M_r$.

Take the time derivative $\dot{V}$ along (10), (11), (14), (16), we have

$$\begin{aligned}\dot{V}&=(z_e-\delta_m)\dot{z}_e+\psi_e\dot{\psi}_e+y_u\dot{y}_u+y_r\dot{y}_r+m_uu_e\dot{u}_e\\&\quad+m_rr_e\dot{r}_e+\tilde{\boldsymbol{W}}_u^{\mathrm{T}}\Gamma_u^{-1}\dot{\hat{\boldsymbol{W}}}_u+\tilde{\boldsymbol{W}}_r^{\mathrm{T}}\Gamma_r^{-1}\dot{\hat{\boldsymbol{W}}}_r\\&\quad+\gamma_{wu}^{-1}\tilde{\tau}_{wu\,\max}\dot{\hat{\tau}}_{wu\,\max}+\gamma_{wr}^{-1}\tilde{\tau}_{wr\,\max}\dot{\hat{\tau}}_{wr\,\max}\\&\le-(k_{ze}-2)(z_e-\delta_m)^2-(k_{\psi e}-2)\psi_e^2\\&\quad-\sum_{i=u,r}\left[\left(\frac{1}{\epsilon_i}-\frac{1}{4}-\frac{M_i^2}{2b}\right)y_i^2+\frac{i_e^2}{2}+\bar{\varepsilon}_i^2\right.\\&\quad+i_e\left(\boldsymbol{W}_i^{\mathrm{T}}\boldsymbol{S}_i-\tau_i-\tau_{wi}\right)+\tilde{\boldsymbol{W}}_i^{\mathrm{T}}\Gamma_i^{-1}\dot{\hat{\boldsymbol{W}}}_i\\&\quad\left.+\gamma_i^{-1}\tilde{\tau}_{wimax}\dot{\hat{\tau}}_{wimax}\right]+b\end{aligned} \tag{21}$$

b is a small positive constant. From Young's inequality, we have

$$\begin{aligned}&|i_e|\tau_{wimax}-\frac{\tau_{wimax}i_e^2}{4\delta_i}\le\delta_i\tau_{wimax},\\&-\tilde{\boldsymbol{W}}_i^{\mathrm{T}}\left(\hat{\boldsymbol{W}}_i-\hat{\boldsymbol{W}}_i(0)\right)\le-\frac{\|\tilde{\boldsymbol{W}}_i\|^2}{2}+\frac{\|\boldsymbol{W}_i-\hat{\boldsymbol{W}}_i(0)\|^2}{2},\\&-\tilde{\tau}_{wimax}(\hat{\tau}_{wimax}-\hat{\tau}_{wimax}(0))\\&\quad\le-\frac{1}{2}\tilde{\tau}_{wimax}^2+\frac{1}{2}(\tau_{wimax}-\hat{\tau}_{wimax}(0))^2\end{aligned} \tag{22}$$

Submitting the control law (17) and adaptive laws (18), (21) yields

$$\begin{aligned}\dot{V}&\le-(k_{ze}-2)(z_e-\delta_m)^2-(k_{\psi e}-2)\psi_e^2\\&\quad-\sum_{i=u,r}\left[\left(\frac{1}{\epsilon_i}-\frac{1}{4}-\frac{M_i^2}{2b}\right)y_i^2+\left(k_{ie}-\frac{1}{2}\right)i_e^2\right.\\&\quad-\tilde{\boldsymbol{W}}_i^{\mathrm{T}}\boldsymbol{S}i_e+|i_e|\tau_{wimax}-\frac{\tau_{wimax}i_e^2}{4\delta_i}-\frac{\tilde{\tau}_{wimax}i_e^2}{4\delta_i}\\&\quad\left.+\tilde{\boldsymbol{W}}_i^{\mathrm{T}}\Gamma_i^{-1}\dot{\hat{\boldsymbol{W}}}_i+\gamma_i^{-1}\tilde{\tau}_{wimax}\dot{\hat{\tau}}_{wimax}+\bar{\varepsilon}_i^2\right]+b\\&\le-(k_{ze}-2)(z_e-\delta_m)^2-(k_{\psi e}-2)\psi_e^2\\&\quad-\sum_{i=u,r}\left[\left(\frac{1}{\epsilon_i}-\frac{1}{4}-\frac{M_i^2}{2b}\right)y_i^2+\left(k_{ie}-\frac{1}{2}\right)i_e^2\right.\\&\quad\left.+\frac{\sigma_i}{2\Gamma_i^{-1}}\tilde{\boldsymbol{W}}_i^{\mathrm{T}}\Gamma_i^{-1}\tilde{\boldsymbol{W}}_i+\frac{\sigma_{wi}\gamma_{wi}}{2}\gamma_{wi}^{-1}\tilde{\tau}_{wimax}^2\right]+\varrho\end{aligned} \tag{23}$$

where

$$\varrho=\sum_{i=u,r}\left[\bar{\varepsilon}_i^2+\delta_i\tau_{wimax}+\frac{\sigma_i}{2}\|\boldsymbol{W}_i-\hat{\boldsymbol{W}}_i(0)\|^2+\frac{\sigma_{wi}}{2}(\tau_{wimax}-\hat{\tau}_{wimax}(0))^2\right]+b.$$

Let

$$a_0=\min\left\{\frac{\sigma_u}{2\lambda_{\max}(\Gamma_u^{-1})},\frac{\sigma_r}{2\lambda_{\max}(\Gamma_r^{-1})},\frac{\sigma wu\gamma_{wu}}{2},\frac{\sigma wr\gamma_{wr}}{2}\right\},$$

and one chose

$$k_{ze}=a_0+2,\quad k_{\psi e}=a_0+2,\quad \frac{1}{\epsilon_i}=a_0+\frac{1}{4}+\frac{M_i^2}{2b},\quad k_{ie}=a_0m_i+\frac{1}{2},\quad i=u,r \tag{24}$$

where a_0 is the positive constant. Then, (23) yields

$$\dot{V}\le-2a_0V+\varrho \tag{25}$$

It follows from (25) that

$$V(t)\le\left(V(0)-\frac{\varrho}{2a_0}\right)e^{-2a_0t}+\frac{\varrho}{2a_0} \tag{26}$$

Based on the closed-loop gain shaping algorithm (Zhang, 2012), inequality (26) confirm that all signals $z_e, \psi_e, u_e, r_e, \hat{\boldsymbol{W}}_u, \hat{\boldsymbol{W}}_r, \hat{\tau}_{wu\,\max}, \hat{\tau}_{wr\,\max}$ are all bounded. With $\lim_{t\to\infty}V(t)=\varrho/2a_0$, there do exist

compact set Ω_Z defined in (19) such that $\boldsymbol{Z} \in \Omega_Z$ for all time. Thus, the state variables of the plant are bounded under the proposed control scheme, i.e.x, y, ψ, u, r.

In the following, one will discuss the bounded dynamics of the sway velocity. The sway dynamics in (1) could be rewritten as follows:

$$\dot{v} = -\frac{m_u}{m_v}ur - \frac{d_v}{m_v}v - \frac{d_{v2}}{m_v}|v|v - \frac{d_{v3}}{m_v}v^3 + \frac{1}{m_v}\tau_{wv} \tag{27}$$

For the marine surface vessel, the inertia and damping parameters $m_u, m_v, d_v, d_{v2}, d_{v3}$ are all with the positive value. Considering the following Lyapunov function candidate:

$$V_v = 0.5v^2 \tag{28}$$

Differentiating Eq. (28) and substituting (27) into it, one can obtain

$$\dot{V}_v = -\left(\frac{d_v}{m_v} + \frac{d_{v2}}{m_v}|v| + \frac{d_{v3}}{m_v}v^2\right)v^2 + \frac{v}{m_v}(\tau_{wv} - m_u ur) \tag{29}$$

Combining with the fact that u and r are uniformly ultimate bounded and τ_{wv} is the bounded disturbance, one can define the upper bound constant B_{ur} satisfying $|\tau_{wv} - m_u ur| \le B_{ur}$. Furthermore, Eq. (29) can be derived as

$$\begin{aligned}\dot{V}_v &\le -\left(\frac{d_v}{m_v} + \frac{d_{v2}}{m_v}|v| + \frac{d_{v3}}{m_v}v^2 - \frac{1}{4m_v}\right)v^2 + \frac{B_{ur}^2}{m_v} \\ &= -\frac{2}{m_v}\left(d_v + d_{v2}|v| + d_{v3}v^2 - \frac{1}{4}\right)V_v + \frac{B_{ur}^2}{m_v}\end{aligned} \tag{30}$$

From (30), it is obvious that $d_v + d_{v2}|v| + d_{v3}v^2$ is increased with the variable $|v|$. If $|v| \ge |\tau_{wv} - m_u ur|/\sqrt{d_v - 1/4}$, then $\dot{V}_v \le 0$. Consequently, one can conclude that the sway dynamics v is also being passive-bounded and further to be uniform ultimate bounded. Therefore, all signals in the closed-loop system are semi-global uniform ultimate bounded.

Remark 4. Note that (24) is just for the stability analysis. If the design parameters are chosen appropriately, $\varrho/(2a_0)$ can be made arbitrarily small, i.e., for any given $\mu > 0$, one has $\lim_{t\to\infty} V(t) \le \mu$.

In this note, the stability result is semi-global in the sense that, for any compact set, there exists a controller with sufficient large number of NNs nodes such that all the closed-loop signals are bounded when the initial states are within this compact set. Different from the existing literatures, the couplings among the state variables and the underactuatedness of marine vessels are considered in the proposed scheme, and a novel guidance system for underactuated ships is developed to reply the marine practical condition.

5. Simulation examples

In this section, we will present two examples to illustrate the effectiveness and merits of the control scheme: Comparative example with the result in Li et al. (2008) and path-following in fields of marine practice. For this purpose, the plant is selected as the underactuated ship (length of 38 m, mass of 118×10^3 kg) in Section 5.1, following Li et al. (2008) and Do and Pan (2006). In Section 5.2, a scientific research vessel YUKUN is considered as the plant to illustrate the more practical test.

5.1. Comparative example with the result in Li et al. (2008)

In this simulation, the proposed adaptive neural controller is compared with the result in Li et al. (2008). The model is represented using (1) and detailed parameters obtained from Li et al. (2008) and Do and Pan (2006), which are assumed to be unknown for the controller. The environmental disturbances are assumed to be $\tau_{wu} = 1.1 \times 10^5[1 + 0.35\sin(0.2t) + 0.15\cos(0.5t)]$, $\tau_{wv} = 2.6 \times 10^5[1 + 0.3\cos(0.4t) + 0.2\sin(0.1t)]$, $\tau_{wr} = 9.5 \times 10^7[1 + 0.3\cos(0.3t) + 0.1\sin(0.5t)]$, that is nonzero-mean time-varying disturbances. The initial conditions are $[x(0), y(0), \psi(0), u(0), v(0), r(0)] = [-80\text{ m}, 20\text{ m}, 0\text{ rad}, 0\text{ m/s}, 0\text{ m/s}, 0\text{ rad/s}]$. The corresponding control parameters also refer to Li et al. (2008). The reference path is generated by the virtual ship (2), $u_d = 6$ m/s, $r_d = \exp(0.005t/300)$ rad/s in the first 30 s and $r_d = 0$ rad/s for 30 s $\le t <$ 70 s, $r_d = 0.05$ rad/s for 70 s $\le t <$ 180 s.

Below, one discusses how to choose control parameters and the number of NNs node. In most control engineering, the performance can be guaranteed by trying a few simulation runs and adjusting the parameters to obtain the good behavior in the practical system. For control parameters, one knows that the control (or adaptive) gains should be large enough to ensure the tracking performance of the closed-loop system and another consideration is that the large parameter setting would lead to unexpected large control signals. Therefore, in general, one first sets large value for the control (or adaptive) gain, and then the parameters should be reduced properly by testing the simulation runs. That can guarantee that the parameter setting is effective in practice. Using the similar procedure, the number of NNs node should be smallest and can be employed to approximate the model uncertainty sufficiently. That would facilitate to apply the proposed algorithm in the practical real-time control. Following the above tuning process, the parameters are taken as (31). The initial values for $\hat{\boldsymbol{W}}_u, \hat{\boldsymbol{W}}_r$ and $\hat{\tau}_{wu\,\max}, \hat{\tau}_{wr\,\max}$ are taken randomly in the interval $(0, 1]$. RBF NNs $\hat{\boldsymbol{W}}_u\boldsymbol{S}_u$ and $\hat{\boldsymbol{W}}_r\boldsymbol{S}_r$ contain 25 nodes. The centers $\boldsymbol{\mu}$ for $[u, v, r, y_u/\epsilon_u]^{\mathrm{T}}$ and $[u, v, r, y_r/\epsilon_r]^{\mathrm{T}}$ both placed in $[-10\text{ m/ s}, 15\text{ m/s}] \times [-5\text{ m/s}, 5\text{ m/s}] \times [-0.6\text{ rad/s}, 0.6\text{ rad/s}] \times [-5, 5]$, the magnification coefficient $\xi_u = 10, \xi_r = 13$, and widths $\eta = 5$:

$$\begin{aligned}&k_{ze} = 2.5, \quad k_{\psi e} = 7, \quad k_{ue} = 3.5 \times 10^5, \quad k_{re} = 6.32 \times 10^9, \\ &\epsilon_u = \epsilon_r = 0.1, \quad \Gamma_u = \mathrm{diag}(2.0), \quad \Gamma_r = \mathrm{diag}(1.4), \\ &\sigma_u = 1.3, \quad \sigma_r = 2.2, \quad \gamma_{wu} = 5.0, \quad \gamma_{wr} = 7.5, \\ &\sigma_{wu} = 0.001, \quad \sigma_{wr} = 0.01, \quad \delta_u = \delta_r = 0.1\end{aligned} \tag{31}$$

The comparative results are given in Figs. 3–5. Fig. 3 shows the path-following trajectory in two-dimensional (2D) plane, where the reference path consists of straight line and a circle. It illustrates that despite the existence of the nonzero-mean time-varying disturbances and unknown model parameters, the path-following control is well established. Figs. 4 and 5 demonstrate the position and orientation errors and the control efforts respectively. Furthermore, one uses two popular performance specifications (32) to evaluate the proposed control scheme, i.e. the mean integral absolute (MIA) value and the mean total variation (MTV) value. t and $t-1$ denote the current sampling time and the past one, respectively. By fusion of these indexes, the comparison performance is measured and summarized

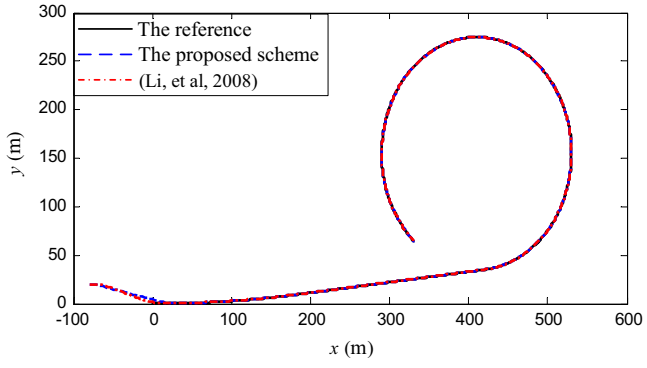

Fig. 3. Path-following trajectory: the proposed algorithm (dashed line) and the result in Li et al. (2008) (dashdotted line).

as Table 1. MIA of the state variables z_e, ψ_e and u_e evaluate the closed-loop performance. MIA and MTV of the control inputs τ_u, τ_r measure the energy cost and the smoothness of the corresponding algorithm. From the above comparisons, the proposed algorithm owns the improved superiority around the control performance and the energy cost aspect. It indicates that the proposed control scheme is more accordance with the engineering requirements:

$$\mathrm{MIA} = \frac{1}{t_\infty - t_0}\int_{t_0}^{t^\infty} |a(t)|\, \mathrm{d}t,$$

$$\mathrm{MTV} = \frac{1}{t_\infty - t_0}\int_{t_0}^{t^\infty} |a(t) - a(t-1)|\, \mathrm{d}t \tag{32}$$

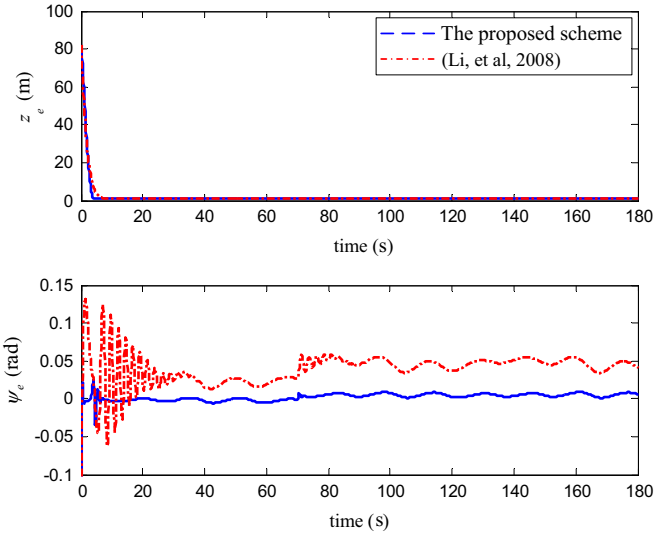

Fig. 4. Position and orientation errors: the proposed algorithm (solid line) and the result in Li et al. (2008) (dashdotted line).

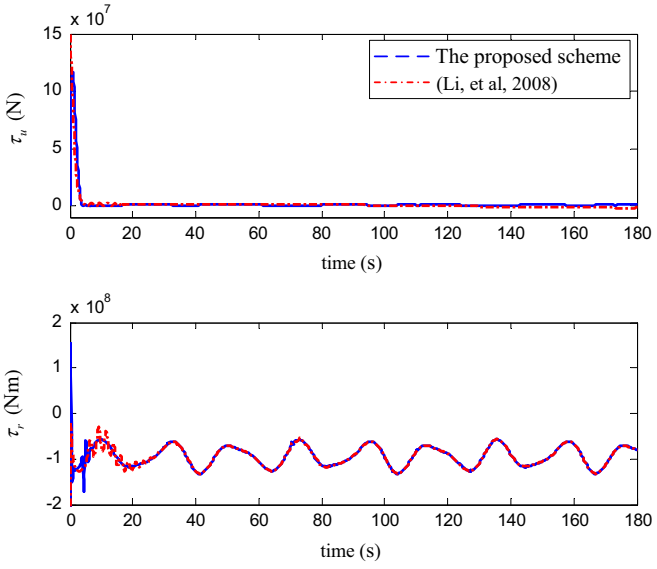

Fig. 5. Control efforts τ_u, τ_r: the proposed algorithm (solid line) and the result in Li et al. (2008) (dashed line).

Remark 5. Figs. 4 and 5 illustrate evident oscillating signals during the initial period of using the proposed algorithm. The main cause is that the tracking errors are large and NNs lack the knowledge about the model uncertainties in the initial phase. Note that the phenomenon is very common for universal adaptive control schemes, e.g., Do and Pan (2006), Ghommam et al. (2010), and Fossen (2005). And the lack of pre-knowledge about the plant hydrodynamics can be lessened by off-line training of the NNs. In addition, in normal ship steering, it often first moves close to the reference path by manual operation, and then switches the autopilot to automatic mode.

5.2. Path-following control in fields of marine practice

To show the superiority of the proposed scheme, the practical test would be compared with the result of Khaled and Chalhoub (2013), where it is a LOS guidance-based control scheme and completes the course-keeping task using a self-tuning fuzzy sliding mode controller. In this section, the plant of interested is the scientific research vessel YUKUN of Dalian Maritime University (DMU), China (see Fig. 6, with length over all 116 m, breadth 18 m and mean draft 5.4 m). Since it is cost-expensive and difficult to test the proposed algorithm using the practical marine vessel, one implements the test confirmation by fusion of the ship motion mathematical model, which is identified from the full-scale trial data. Fig. 7 presents the comparison result of the neural simulation and the full-scale turning trail $\delta = -20^\circ$. Certainly, the other trials also have been conducted for the confirma-

Fig. 6. The vessel YUKUN of Dalian Maritime University.

Table 1
Control performances of the proposed algorithm and the result in Li et al. (2008).

Indexes	MIA			
Variables	z_e		ψ_e	u_e
Control law (18)	1.1790		0.0402	0.1120
Li et al. (2008)	1.7601		0.0677	0.4844
Indexes	MIA		MTV	
Variables	τ_u	τ_r	τ_u	τ_r
Control law (18)	1.0282E6	9.2969E7	3.8999E4	8.3981E5
Li et al. (2008)	2.4433E6	9.4395E7	6.2701E4	1.3408E6

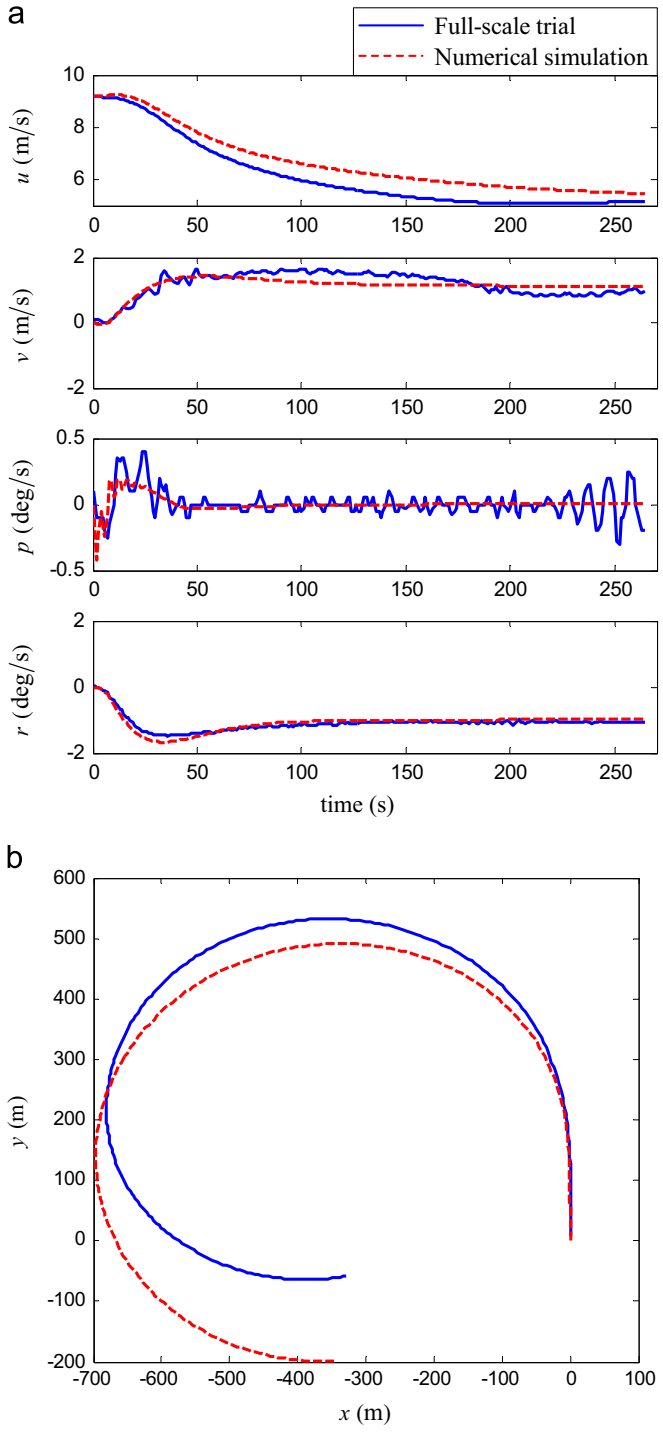

Fig. 7. Comparison of the numerical simulation and the full-scale turning trail $\delta = -20^{\circ}$: (a) the kinematic variables; (b) the movement trajectory.

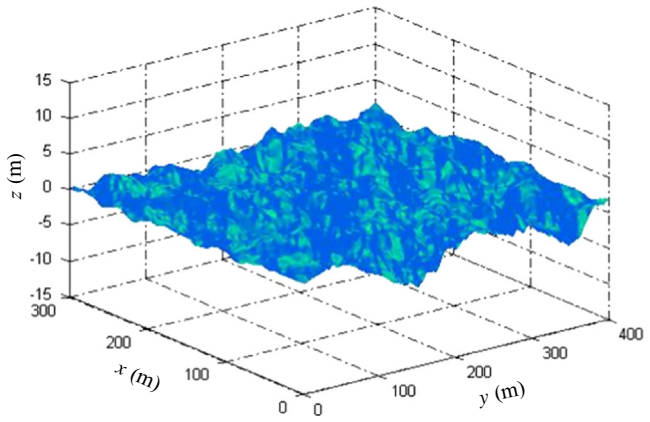

Fig. 8. Graph of the irregular waves with the 6th level sea state.

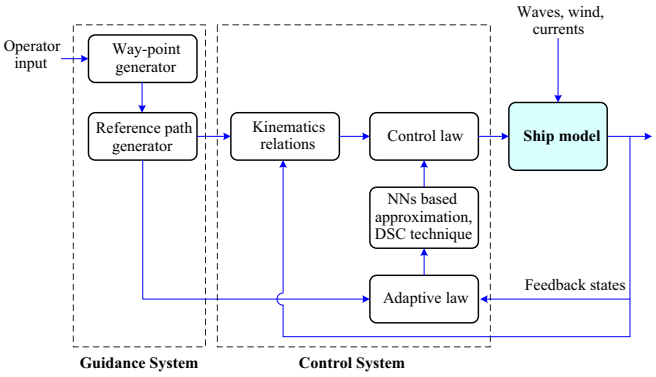

Fig. 9. Conceptual signal flow box diagram for simulation.

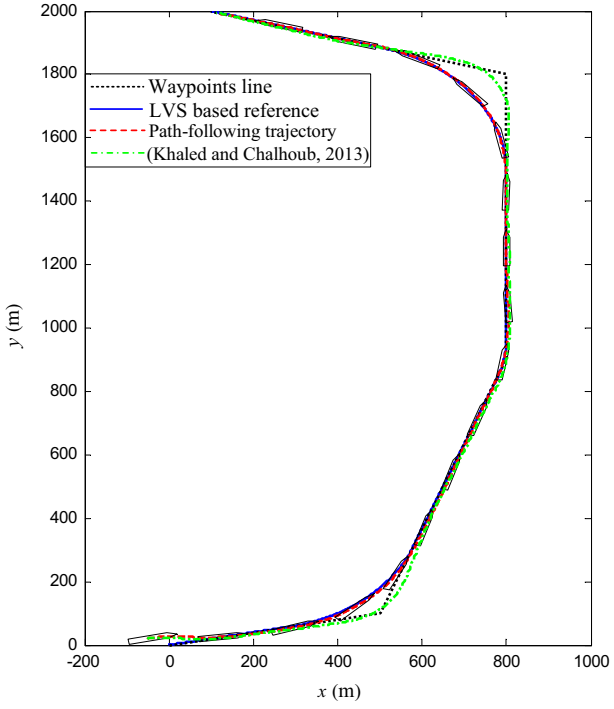

Fig. 10. Path-following trajectory in fields of marine practice: the proposed scheme (solid line) and the result in Khaled and Chalhoub (2013) (dashdotted line).

tion, e.g. the zigzag manoeuvring simulation. They would not be presented here due to the limited space. These comparison results indicate that the mathematical model could accurately describe 4 degrees of freedom (DOF, including the surge, sway, roll and yaw motions) dynamic response of vessel YUKUN. For details about the hydrodynamic terms, refer to Table A1. Note, the hydrodynamic terms are unknown for the controller design, as well as the unmodeled dynamics. The model is only for the test plant. For the consideration of marine practice, the waypoints based planed route consists of waypoints $W_1(0,0), W_2(100,500), W_3(900,800), W_4(1800,800)$ and $W_5(2000,100)$, with the units m. The desired speed $u_d = 8.5$ m/s. The marine environmental disturbances include wind, irregular wind-

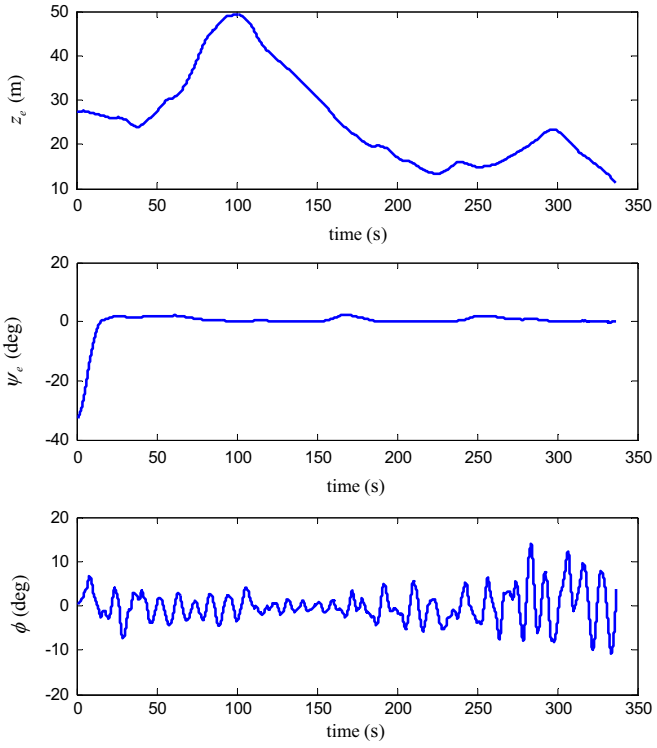

Fig. 11. Position error, orientation error and the roll angle in fields of marine practice.

generated wave and ocean currents. Those are simulated by virtue of the physical based model detailed in Fossen (1998, 2011).

In the experiment, the wind speed (Beaufort No.6) $V_{\text{wind}} = 12.3$ m/s, wind direction $\psi_{\text{wind}} = 230^\circ$, and the Pierson–Moskowitz (PM) spectrum is chosen to produce the wind-generated waves. Fig. 8 shows the wave graphs with the 6th level sea state. The current speed $V_{\text{current}} = 1$ Kn and current direction $\beta_{\text{current}} = 280^\circ$. The initial states of vessel YUKUN is $[x(0), y(0), \phi(0), \psi(0), u(0), v(0), p(0), r(0)] = [-50\text{ m}, 20\text{ m}, 0^\circ, 0^\circ, 8\text{ m/s}, 0\text{ m/s}, 0^\circ/\text{s}, 0^\circ/\text{s}]$, where ϕ and p denote the roll angle and rolling rate, respectively. Fig. 9 demonstrates the conceptual signal flow box diagram for the path-following control scheme. Because the vessel YUKUN is different from the underactuated vehicle in Section 5.1, the control parameters setting is adjusted as Eq. (33). In order to illustrate the generalization and robust performance of RBF NNs $\hat{\boldsymbol{W}}_u\boldsymbol{S}_u$ and $\hat{\boldsymbol{W}}_r\boldsymbol{S}_r$, the parameter setting follows the details of Section 5.1. Since the vessel YUKUN differs from the plant (Khaled and Chalhoub, 2013), the control parameter for the LOS guidance-based algorithm follows Khaled and Chalhoub (2013) except the modification of $\lambda_s = 6$, $\Phi_s = 0.04$, $\lambda_h = 0.1$, $\Phi_h = 0.01$:

$$
\begin{aligned}
&k_{ze} = 1.5, \quad k_{\psi e} = 5, \quad k_{ue} = 5.5 \times 10^5, \quad k_{re} = 2.35 \times 10^7,\\
&\epsilon_u = \epsilon_r = 0.1, \quad \Gamma_u = \text{diag}(2.0), \quad \Gamma_r = \text{diag}(1.4),\\
&\sigma_u = 1.3, \quad \sigma_r = 2.2, \quad \gamma_{wu} = 5.0, \quad \gamma_{wr} = 7.5,\\
&\sigma_{wu} = 0.001, \quad \sigma_{wr} = 0.01, \quad \delta_u = \delta_r = 0.1
\end{aligned} \tag{33}
$$

Figs. 10–12 present the path-following control results of vessel YUKUN in fields of marine practice. From Fig. 10, it is obvious that the proposed control scheme could effectively avoid the overshoot existed in the current theoretical works, which is mainly caused by the large inertia of marine vessel. With the valid control action both in the straight line and curved segment, the control performance is reasonable and effective from the view point of practice. Fig. 11 details the position and orientation errors and the roll angle. Although the error z_e always does not convergent to zero, that is acceptable for the marine vessel of 116 m length. In

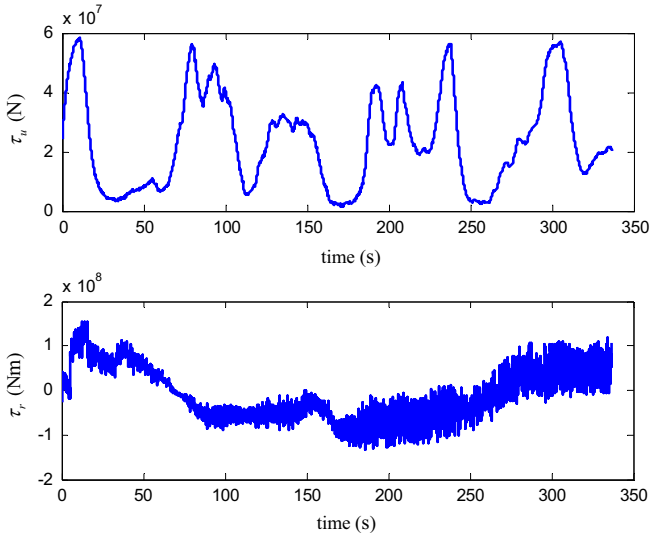

Fig. 12. Control efforts τ_u, τ_r in fields of marine practice.

addition, the roll angle in Fig. 11 demonstrates that the roll motion is excited mainly by the irregular waves and less component is from the effect of the control input τ_r. For the research topic of this note, analysis around the roll motion is not detailed. In Fig. 12, it is noted that the chatter drawn of τ_r may not be realistic. In fact, the considered mathematical model is constructed without modules to describe the marine main engine and the rudder servo machine. That is the main factors to cause the chattering, since the rudder servo system has the filtering effectiveness from the rudder angle to the yaw moment. Therefore, the phenomenon would not appear in the marine control engineering. Motivated by the above analysis, the numerical result has shown the good performance of the proposed scheme.

6. Conclusions

In this paper, one focuses on path-following control for underactuated ships in fields of marine practice. A novel LVS guidance system law is first developed to tackle the practical condition: the reference path generated by waypoints. Furthermore, an adaptive neural path-following control scheme is presented by virtue of nonlinear function approximation, DSC technique and polar coordinates, and the SGUUB stability of the closed-loop system has been proved using Lyapunov theory. Compared with the existed literature, the control performance is more accordance with the engineering requirements for the merits of these new techniques. Simulation results have been presented to illustrate the performance and the effectiveness of the proposed algorithm, which can also be used for the other practical underactuated system such as the nonholonomic mobile robot.

Even though, this work cannot attend to every detail of the control task, e.g., the algorithm may not targetly account for saturation of the control actions. That would be the further problem to be solved in the following works.

Acknowledgments

This work is partially supported by the National Natural Science Foundation of China (Grant nos. 51109020, 51409033), and the Fundamental Research Funds for the Central University (Grant no. 2014YB01; 3132014302).

Appendix A. Model parameters for vessel YUKUN

See Table A1.

Table A1
The non-dimensional hydrodynamic coefficients for the vessel YUKUN in Section 5.2.

Structure for the hydrodynamic force (or moment)

$X: u^2, u^3, v^2, r^2, vr, uv^2, uv\phi^2$

$Y: uv, up, u^2v, r^3, vr^2, v^2r, uvp^2, urp^2, |v|v, |r|v, |v|r, |r|r$

$K: p, uv, ur, u^2v, v^3, vr^2, v^2r, uv\phi^2, ur\phi^2, |v|v$

$N: uv, up, u\phi, u^2r, u^2v, v^3, r^3, vr^2, v^2r, urp^2, |v|v, |r|v$

The hydrodynamic coefficients normalized using the Prime-system I

$X'_{uu} = 0.0004$	$Y'_{urpp} = 0.1464$	$K'_{\|v\|v} = 0.0006$
$X'_{uuu} = -0.0003$	$Y'_{\|v\|v} = -0.1068$	$N'_{uv} = 0.0070$
$X'_{vv} = 0.3285$	$Y'_{\|r\|v} = -0.0384$	$N'_{up} = -0.0007$
$X'_{rr} = -0.0024$	$Y'_{\|v\|r} = 0.0334$	$N'_{u\phi} = -0.0016$
$X'_{vr} = -0.0111$	$Y'_{\|r\|r} = 0.0274$	$N'_{uur} = -0.0004$
$X'_{uvv} = -0.3364$	$K'_{p} = -1.66E-5$	$N'_{uuv} = -0.0099$
$X'_{uv\phi\phi} = 0.2984$	$K'_{uv} = -0.0025$	$N'_{vvv} = -0.0419$
$Y'_{uv} = 0.3609$	$K'_{ur} = -0.0001$	$N'_{rrr} = 0.0001$
$Y'_{up} = 0.0098$	$K'_{uuv} = 0.0024$	$N'_{vrr} = -0.0132$
$Y'_{uuv} = -0.3538$	$K'_{vvv} = 0.0246$	$N'_{vvr} = 0.0209$
$Y'_{rrr} = -0.0202$	$K'_{vrr} = 0.0072$	$N'_{urpp} = 0.0101$
$Y'_{vrr} = 0.1275$	$K'_{vvr} = 0.0225$	$N'_{\|v\|v} = 0.00210$
$Y'_{vvr} = -0.1460$	$K'_{uv\phi\phi} = 0.0832$	$N'_{\|r\|v} = 0.0126$
$Y'_{uvpp} = -0.2518$	$K'_{ur\phi\phi} = 0.0109$	

References

Breivik, M., Hovstein, V.E., Fossen, T.I., 2008. Ship formation control: a guided leader-follower approach. In: IFAC World Congress, pp. 16008–16014.

Brockett, R., Millman, R., Sussman, H., 1983. Differential Geometric Control Theory. Birkhauser, Boston.

Chen, M., Ge, S.S., Choo, Y.S., 2009. Neural network tracking control of ocean surface vessels with input saturation. In: Proceedings of the IEEE International Conference on Automation and Logistics, Shenyang, China, pp. 85–89.

Chen, W., Jiao, L., 2010. Adaptive tracking for periodically time-varying and nonlinearly parameterized systems using multilayer neural networks. IEEE Trans. Neural Netw. 21, 345–351.

Chen, M., Ge, S.S., Cui, R., 2010a. Adaptive nn tracking control of overactuated ocean surface vessels. In: Proceedings of the 8th World Congress on Intelligent Control and Automation, Jinan, China, pp. 548–552.

Chen, W., Jiao, L., Li, R., Li, J., 2010b. Adaptive backstepping fuzzy control for nonlinearly parameterized systems with periodic disturbances. IEEE Trans. Fuzzy Syst. 18, 674–685.

Do, K.D., 2010. Practical control of underactuated ships. Ocean Eng. 37, 1111–1119.

Do, K.D., Jiang, Z.P., Pan, J., 2004. Robust adaptive path following of underactuated ships. Automatica 40, 929–944.

Do, K.D., Pan, J., 2006. Underactuated ships follow smooth paths with integral actions and without velocity measurements for feedback: theory and experiments. IEEE Trans. Control Syst. Technol. 14, 308–322.

Do, K.D., Pan, J., 2009. Control of Ships and Underwater Vehicles—Design of Underactuated and Nonlinear Marine Systems. Springer, New York.

Fossen, T.I., 1998. Guidance and Control of Ocean Vehicles. Wiley, New York.

Fossen, T.I., 2005. A nonlinear unified state-space model for ship maneuvering and control in a seaway. J. Bifurc. Chaos 32, 1486–1502.

Fossen, T.I., 2011. Handbook of Marine Craft Hydrodynamics and Motion Control. Wiley, New York.

Ge, S.S., Hang, C.C., Lee, T.H., Zhang, T., 2001. Stable Adaptive Neural Network Control. Kluwer Academic Publisher, Norwell, USA.

Ge, S.S., Wang, C., 2002. Direct adaptive nn control of a class of nonlinear systems. IEEE Trans. Neural Netw. 13, 214–221.

Ghommam, J., Mnif, F., Benali, A., Derbel, N., 2006. Asymptotic backstepping stabilization of an underactuated surface vessel. IEEE Trans. Control Syst. Technol. 14, 1150–1157.

Ghommam, J., Mnif, F., Derbel, N., 2010. Global stabilisation and tracking control of underactuated surface vessels. IET Control Theory Appl. 4, 71–88.

Jiang, Z.P., 2002. Global tracking control of underactuated ships by Lyapunov's direct method. Automatica 38, 301–309.

Jiang, Z.P., 2011. Controlling underactuated mechanical systems: a review and open problems. In: Lecture Notes in Control and Information Sciences, vol. 407, pp. 77–88.

Khaled, N., Chalhoub, N.G., 2013. A self-tuning guidance and control system for marine surface vessels. Nonlinear Dyn. 73, 897–906.

Krstic, M., Kanellakopoulos, I., Kokotovic, P., 1995. Nonlinear and Adaptive Control Design. Wiley, New York.

Li, J.H., Lee, P.M., Jun, B.H., Lim, Y.K., 2008. Point-to-point navigation of underactuated ships. Automatica 44, 3201–3205.

Li, T.S., Li, R.H., Wang, D., 2012. Adaptive neural control of nonlinear MIMO systems with unknown time delays. Neurocomputing 78, 83–88.

Li, T.S., Wang, D., Feng, G., Tong, S.C., 2010. A DSC approach to robust adaptive NN tracking control for strict-feedback nonlinear systems. IEEE Trans. Syst. Man Cybern. 40, 915–927.

Liu, Z., Yu, R., Zhu, Q., 2012. Comments on asymptotic backstepping stabilization of an underactuated surface vessel. IEEE Trans. Control Syst. Technol. 20, 286–288.

Peng, Z., Wang, D., Hu, X., 2010. Robust adaptive formation control of underactuated autonomous surface vehicles with uncertain dynamics. IET Control Theory Appl. 5, 1378–1387.

Pettersen, K.Y., Nijmeijer, H., 2001. Underactuated ship tracking control: theory and experiments. Int. J. Control 74, 1435–1446.

Tee, K.P., Ge, S.S., 2006. Control of fully actuated ocean surface vessels using a class of feedforward approximators. IEEE Trans. Control Syst. Technol. 14, 750–756.

Ting, C., 2009. An output-feedback fuzzy approach to guaranteed cost control of vehicle lateral motion. Mechatronics 19, 304–312.

Tong, S., Liu, C., Li, Y., 2010. Fuzzy-adaptive decentralized output-feedback control for large-scale nonlinear systems with dynamical uncertainties. IEEE Trans. Fuzzy Syst. 18, 845–861.

Wang, D., Huang, J., 2005. Neural network-based adaptive dynamic surface control for a class of uncertain nonlinear systems in strict-feedback form. IEEE Trans. Neural Netw. 16, 195–202.

Yang, Y., Wang, X., 2007. Adaptive NN tracking control for a class of uncertain nonlinear systems using radial-basis-function neural networks. Neurocomputing 70, 932–941.

Yang, Y., Zhou, C., 2005. Robust adaptive fuzzy tracking control for a class of perturbed strict-feedback nonlinear systems via small-gain approach. Inf. Sci. 170, 211–234.

Zhang, X., 2012. Ship Motion Concise Robust Control. Science, Beijing.